Numerical Methods in Civil Engineering, 8-4 (2024) 20-39

Numerical Methods in Civil Engineering

Journal Homepage: https://nmce.kntu.ac.ir/

Evaluation of ground motion amplification across empty valleys subjected to inclined SV waves using boundary element method

Ehsan Nafici*, Behrouz Gatmiri**

ARTICLE INFO

RESEARCH PAPER

Article history:
Received:
September 2023
Revised:
October 2023
Accepted:
January 2024

Keywords:
Topographical effects,
HYBRID,
2D site effect,
oblique SV waves,
empty valleys.

Abstract:

Many recorded earthquakes in last few decades have shown that the damage distribution and seismic response of an area depend on source characteristics, the pathway of seismic waves, and also on local site conditions; These conditions can change the amplitude of displacement and the frequency properties of ground movement. Local site effects include geotechnical and topographical effects. Unfortunately, most modern seismic codes consider geotechnical effects, and those that consider topographical effects focus on simple geometries. However,other parameters such as wave characteristics are not taken into account. The main reason is the lack of quantitative amplification predicting methods and practical information in topography constructions. The present study evaluates 2D seismic site effects in empty valleys. Numerical analysis is carried out using HYBRID software. HYBRID is a nonlinear, two-phase, code for solving 2D problems of propagation of the waves; this software combines F.E.M in the near field and B.E.M in the far field. Empty valleys are modeled, with different shapes, including rectangle, triangle and trapezoid and with depth ratios equal to 1, 0.8, 0.6, 0.4, and 0.2. Oblique SV waves of Ricker type are considered seismic solicitation and their angle of incidence varies from -90º to 90º every 10º. It is shown that the incidence angle can change the maximum amplification and the critical incidence angle of a half-space is changed by topography.

1. Introduction

Many pieces of recorded evidence of historical earthquakes are available to prove the significant local site effects on the distribution and level of destruction [1,2]. Among them are the 1989 Loma Prieta earthquake [3], the 1994 Northridge earthquake [4,5], the 1995 Egion earthquake [6] and the 1999 Athens earthquake [7]. Additionally, extreme accelerations reported at Pacoima dam (1.25g) as real instrumental evidence without destruction during San Fernando earthquake is [8]. It is generally recognized that seismic site effects are caused by topographic irregularities, the order of soil layers, the morphology of stratigraphic contacts, and the dynamic properties of the soils, which affect the wave propagation process [9-13]. Thus, the presence of a large irregularity like a canyon, ridge, hill, or slope changes the amplitude and frequency content of dimensional site effects which include the thickness and ground movement. Current seismic codes such as NEHRP 1994, 1997, IBC2000, and UBC1997 consider one- some characteristics of a homogenous sedimentary layer, moreover, wave propagation is assumed to be in a vertical direction [14].

A large number of studies have addressed topography issues based on different techniques [15,16]. Different points of view are used to categorize and review these investigations. Through a very frequently using classification, site effect studies are assumed to be conducted via experimental approach, analytically solved wave propagation problems, numerical analyses and empirical methods [17] (occasionally based on the problem limitations and available facilities) as presented in the following.

Experimental estimation of site effects may be an alternative to represent what happens in real where other methods are not yet efficient enough to assess. it is divided into two main branches [18]: 1) reference site methods (RSM), in which a station in the absence of site effects is taken to form the classical spectral ratio; it has some subdivision methods too [19-21] and much work has done yet based on it [22-24]. 2) nonreference site methods which are especially suitable when finding a reference point is impossible [18]. As an

** Corresponding Author: Graduated Student in Geotechnical Engineering, Department of Civil Engineering, College of Engineering, University of Tehran, 16 Azar St., Enghelab St., Tehran, Iran, Email: Ehsannafici@ut.ac.ir*

*** Full Professor, Department of Civil Engineering, College of Engineering, University of Tehran, Email: Gatmiri@ut.ac.ir*

https://doi.org/10.61186/NMCE.2303.1031

example, the horizontal-to-vertical spectral ratio (H/V) needs one station and employs vertical displacement as a reference. This method was introduced first by Nogoshi and Igarashi (1970) [25], popularized by Nakamura (1989) to study site response of S waves [26] and developed theoretically by Lermo and Chavez-Garcia (1993) using numerical modeling of SV waves [27] and applied in several publications using both earthquake waves and seismic noises [28-31].

Although the analytical approach is a closed-form solution for wave propagation problems, various complexities such as the geology, topography shapes and different wave types restrict this method from being applied to predict ground motion only in some simplified conditions and is used as a verification criterionto prove the capability of their own investigative methods [32]. One primary work in this field is the calculation of elastic wave motion in an isotropic half-space when a point load is applied, as done by Lamb [33] in 1904. Years after that, the problem was solved for a layered half-space using Green's function [34,35] and Garvin [36] solved the problem for a line-load on an isotropic half-space. In 1950 Thomson introduced a matrix formulation technique for wave propagation in a layered medium [37]. Haskell Improved the formulations in 1953,1962 and 1963[38-41], therefore, the transfer matrix method became a systematic solution for governing equations in elastodynamic problems in a layered medium, and it was used several times by many researchers since then.

There are three main numerical methods: domain methods, boundary methods, and hybrid methods. Each of them has certain advantagesover the others when used in a correct condition.

The most frequently used domain methods to study topography effects are finite element methods (FEM) and finite difference methods (FDM). The FDM is easy to use, and its low calculation cost is an advantage, but it is hard to use in geometrically complicated problems [42]. The approach was initially used by Alterman and Karal in 1968 to work on the propagation of waves in elastic media [43] and was used several times after [44-46].

Aki and Larner were pioneers in boundary methods. In 1970 they introduced a semi-analytical/semi-numerical method [47] according to the formulation of Rayleigh for wave scattering in a layered medium. Boundary methods have been widely used by researchers. Bard and Bouchon (1980) [48,49] utilized this method to study sedimentary basins under P, SV, and SH waves. Geli et al. (1988) [50] employed this method in their numerical studies. Furthermore, Bouchon (1973) [51] and Bard (1982) [52] used this method to investigate the two-dimensional site effects. In accordance with the BEM framework, the dimensionality of the problem is decreased by one. Additionally, it is feasible to precisely accommodate radiation boundary conditions, in the presence of a suitable Green's function.

A combination of two methods generates a hybrid method [53-62]. In 2002, Gatmiri et al. expanded the combination of the FEM and the BEM in a computer program called HYBRID to investigate the seismic response of two-dimensional porous dry and saturated media [63-65]. Several topographies with different geological and geometrical conditions have been investigated by HYBRID code till now [66-76] but seismic waves have been considered to propagate vertically in most of them, for example: Le Pense et al. in 2011 [72] conducted a comparison between two-dimensional and one-dimensional site response. They initially obtained the amplification of a sediment layer placed on a half-space and compared and saw a match with analytical solution. Then, a criterion for classifying the 1D soil layer responses based on thickness and impedance ratio was proposed by them. Gatmiri and Foroutan conducted parametric studies on empty, full, and half-full alluvial valleys in 2012 [73] and classified valleys according to shape, depth ratio and impedance ration. Kamalian et al. 2007 investigated the seismic behavior of homogeneous and heterogeneous dual composite hills against vertical shear waves using the boundary element method in the time domain [74]. Gatmiri and Amini in 2014 highlighted the importance of considering the shape and mechanical properties of sediment-filled valleys in assessing seismic hazards [75] and Gatmiri et al. gave some practical recommendations on this subject [76].

In this paper the incidence angle of seismic SV waves combined with geometrical parameters in empty valleys have been studied. HYBRID code is used as the numerical method [63-65], different shapes of valleys including rectangle, trapezoid and triangle have been modeled and various graphs presented and discussed as the results.

2. Model setup

2.1 Numerical method

HYBRID code, developed by Gatmiri et al. in 2000 [63-65] uses FEM in the near field and BEM in the far field is used as the numerical method to calculate displacements across the valleys subjected to oblique SV waves.

2.2 Geometrical Parameters

The valleys are assumed to be free of sediments and take the form of rectangles, trapezoids, and triangles. The geometry of the valleys is shown in Figure 1, L equals to 100 m for all shapes, the dimensionless parameter H/L is called depth ratio and is taken 0.2, 0.4, 0.6, 0.8, and 1 for all three shapes and the L_1/L parameter for rectangular, and trapezoidal and triangular valleys is taken 1, 0.4 and 0 respectively.

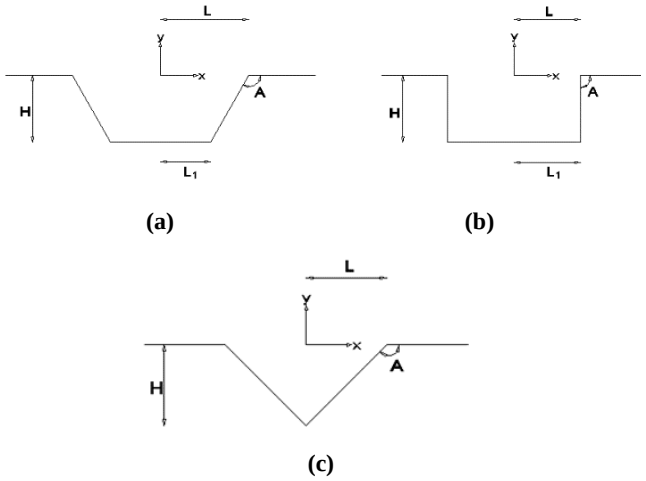

Fig. 1: Geometrical characteristics of the valleys. **(a)** trapezoid; **(b)** rectangle; **(c)** tringle

2.3 Incident wave characteristics

Oblique SV waves of Ricker walvet type wave is considered in all models as a seismic signal, the equation (1) expresses the displacement imposed by the signal.

$$U(t) = A_0(a^2 - 0.5)e^{-a^2} \quad (1)$$

$$a = \pi \frac{t - T_s}{T_p} \quad (2)$$

In equation (2) A_0, T_s and T_p are considered 1, 0.5 and 0.5 respectively and the displacement diagram of the wave is shown in Figure 2.

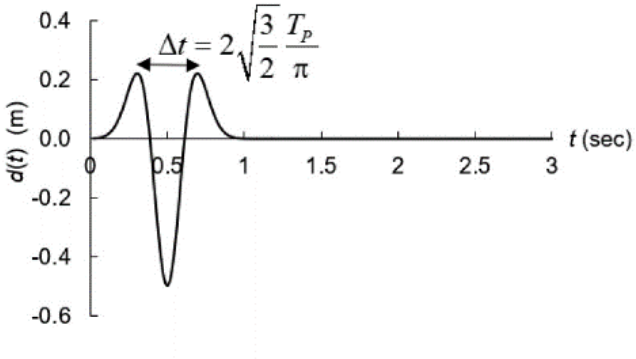

Fig. 2: imposed displacement of Ricker wave

The incidence angle of the waves is shown by α and measured with respect to the vertical axis, ranging from -90 to 90 degrees, with a 10-degree interval.

2.4 Mechanical parameters of the materials

The material of the bedrock is assumed to be dry, linear elastic and homogeneous and the mechanical properties are shown in table 1.

Table 1: mechanical characteristics

E (Mpa)	υ	ρ (kg/m^3)	C (m/s)
6720	0.4	2400	1000

3. Results

3.1 The effect of incidence angle of the waves on amplification across the valley

According to the symmetry of the models, the two-dimensional response of a point at a distance of x from the center of the valley and the incidence angle of α equals the response of a point at the distance of -x and the angle of -α. Therefore, by representing half of the valley at incidence angles ranging from -90 to 90 degrees, the response of all points within the valley can be obtained. the positive direction of the incident wave angle and the distance from the center is considered according to Figure 3.

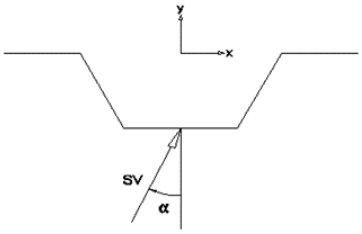

Fig. 3: The Positive incidence angle and distance from the center

The amplification (Am) at a point is calculated as the ratio of the total displacement (resultant of horizontal and vertical displacements) at that point to the total displacement at a point far from the valley (no topographic effect).

The Am graphs of the total displacement for different points in empty valleys are shown in the Appendix.

• In each of the three shapes, rectangle, trapezoid, and triangle, each angle of wave incidence and at each depth the maximum amplification is seen at the edge of the valley. The magnitude of amplification varies with the change in angle of wave incidence and the depth ratio.

• The variations trend of amplification with changes in angle of wave incidence are nearly similar for positive and negative angles but differ in magnitude.

• The amplification pattern which Can be seen moving from the center of the valley towards the edge, varies with different angles of wave incidence. In some angles, Am increases as it moves from the center towards the edge (behavior 1), while in some angles it decreases (behavior 2).

3.2 Combined effects of angularity of incident wave and offset

In Figure 4, if Am (center) - Am (down edge) is positive, behavior 1 occurs, and if it is negative, behavior 2 occurs. This actually indicates the combined effect of the angle of wave radiation and offset. Regarding triangular valleys, due to the absence of a horizontal bottom surface (the center and lower edge of the valley are aligned), the mentioned graph is plotted as the difference between the upper and lower edges of the valley, and it is observed that they exhibit

behavior similar to ridges [66]. In other words, triangular valleys exhibit behavior 2 in almost all angles of wave incidence.

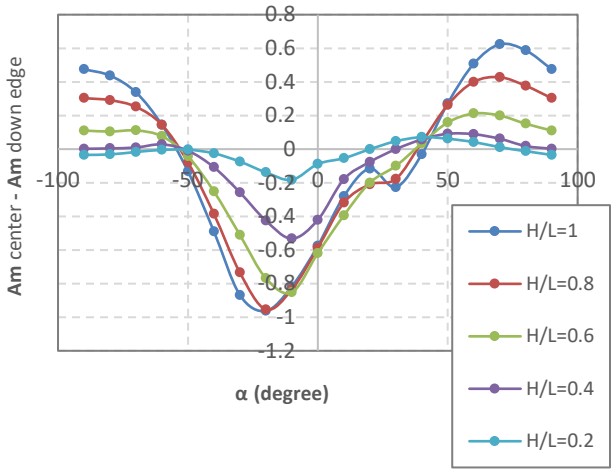

(a)

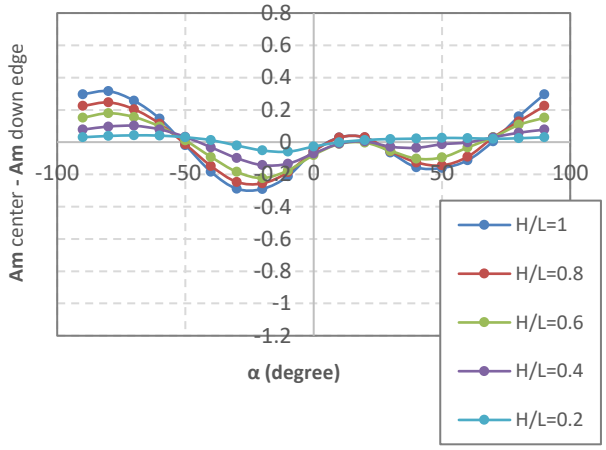

(b)

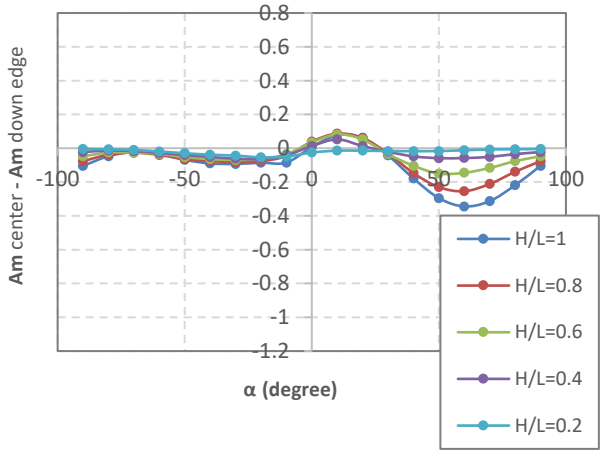

(c)

Fig. 4: variation of ($A_{center} - A_{down\ edge}$) as a function of (α), **(a)** rectangle; **(b)** trapezoid; **(c)** triangle

3.3 Evaluation of critical points

The influence of various parameters on displacement amplification has been investigated at the edge of valleys. The edge is identified as the most critical point in all cases, and the center of the valley, which typically has the minimum Am value, has been investigated in the following.

3.3.1 The edge of the valley

3.3.1.1 Effect of incidence angle of the waves

The amplification diagram for empty valley edges is shown in Figure 5. The following results can be observed:

• In all three valley shapes and at any depth ratio, the maximum amplification occurs at an angle of approximately 10 degrees.

• The magnification value increases with an increase in the depth ratio for any angle of wave incidence, α.

• The rate of changing Am (as a function of α) increases, as the depth ratio increases.

• As the angle deviates from 10 degrees, the amplification value decreases, but an increase in Am is observed as α approaches 90 degrees (more pronounced in triangular shapes) which is smaller than the maximum Am. This effect intensifies with the influence of topography [66], resulting in a greater increase in rectangular shapes than trapezoidal shapes, and greater in trapezoidal shapes than triangular shapes.

3.3.1.2 Combined effects of angularity and depth ratio

Two following effects on the variations in depth ratio are clearly observable:

• At any angle of wave incidence, the amplification value increases with an increase in the depth ratio, and the rate of enhancement decreases as the incidence angle deviates from the maximum Am, which is approximately 10 degrees. This observation can be seen in Figure 5.

• The influence of the angle of wave incidence on the variations in amplification increases with an increase in the depth ratio. To illustrate, Figure 6 shows the maximum variations in Am within the range of -90 to 90 degrees against the depth ratio.

3.3.2 The center of the valley

3.3.2.1 Effects of the incidence angle of the waves

The graph of amplification versus wave incidence angle for the center of empty rectangular, trapezoidal, and triangular-shaped valleys is shown in Figure 7, and the following observations can be made:

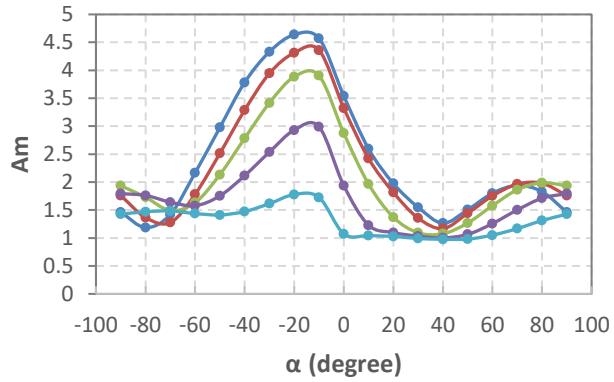

(a)

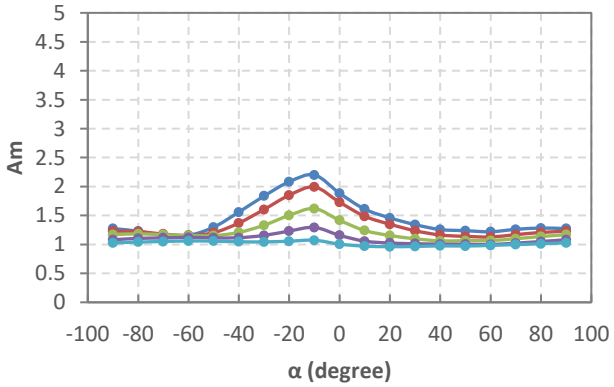

(b)

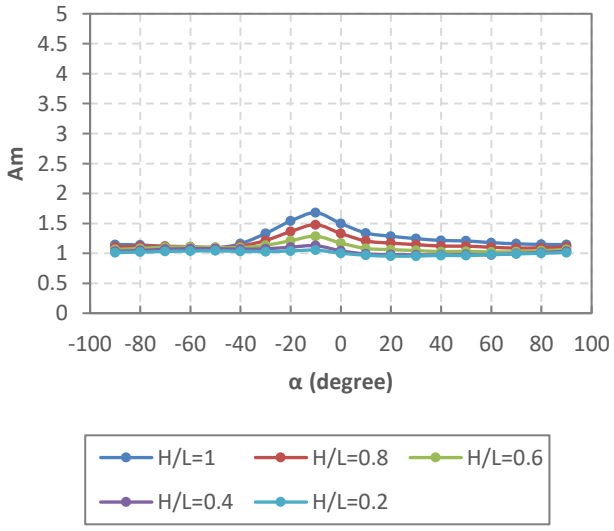

(c)

Fig. 5: The amplification of the edge of empty valleys as a function of incidence angle: (a) rectangle, (b) trapezoid, (c) triangle

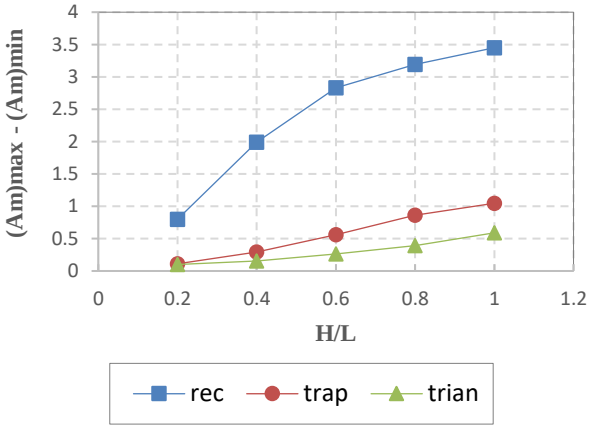

Fig. 6: The maximum change in amplification at the edge of valleys as a function of depth ratio

• The amplification value initially decreases with an increase in α up to a certain angle, after which it begins to increases. This angle increases with an increase in the depth ratio. If this angle is denoted by λ, the graph of λ versus depth ratio is presented in Figure 8.

• There exists an angle in rectangular valleys where the Am is equal to one for all depth ratios. If we denote this angle as **Ω**, its value is 55 degrees for rectangular valleys, 80 degrees for trapezoidal valleys, and approaches infinity for triangular valleys from a mathematical perspective; however, this does not have a physical interpretation. In other words, as the topographic effect decreases, the angle **Ω** increases.

3.3.2.2 Combined effects of angularity and depth ratio

• for angles smaller than **Ω**, de-amplification intensifies as the depth ratio increases. For angles larger than **Ω**, amplification increases as the depth ratio goes up (there are few exceptions in rectangular shape valleys)

• Similar to the edges of valleys, the maximum amplification change occurring at the center is plotted against the depth ratio in Figure 9, and it is observed that the effect of wave incidence angle on amplification variations increases with an increase in the depth ratio.

3.4 Critical incidence angle concept

In technical literature, the critical incidence angle is a concept thatrefers to the angle at which the incidence of SV waves into a half-space causes a sudden increase in horizontal displacement amplification. The value of this angle can be calculated using equation (3) for elastic materials.

$$\theta_{critical} = sin^{-1}\left(\frac{1-2\upsilon}{2(1-\upsilon)}\right) \quad (3)$$

For the materials used in the half-space where the investigated topographies are present, this angle is equal to 24 degrees. Many studies have considered the effects of SV wave generation at the critical incidence angle (such as Kawazoe and Aki in 1990 [36]).

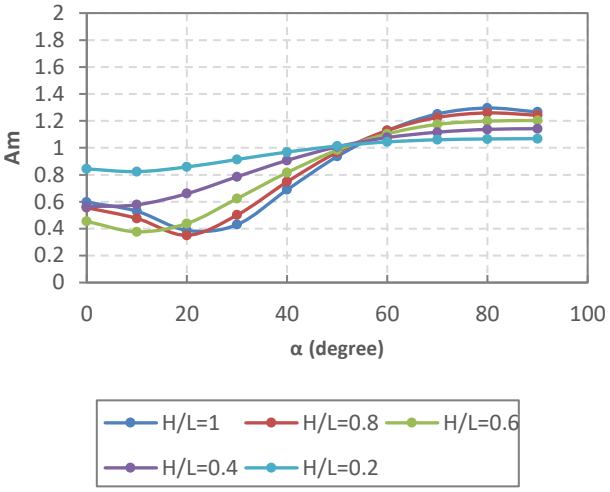

(a)

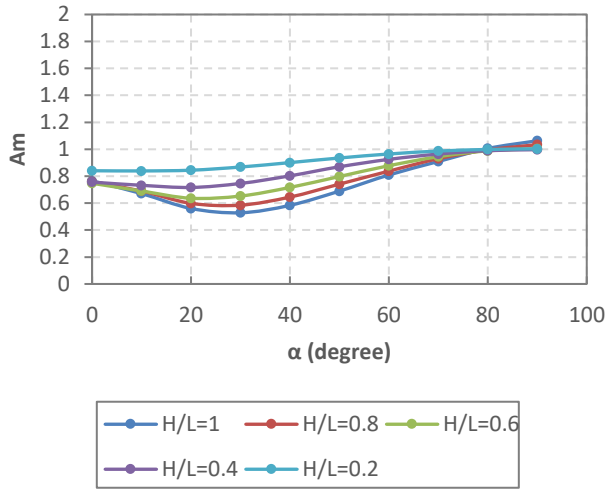

(b)

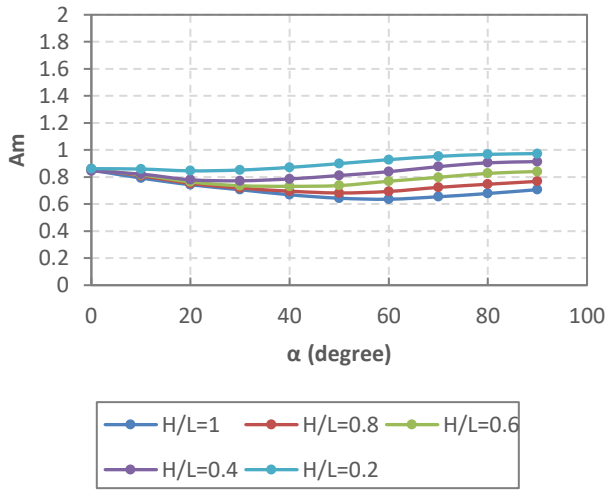

(c)

Fig. 7: The amplification at the center of empty valleys as a function of wave incidence angle

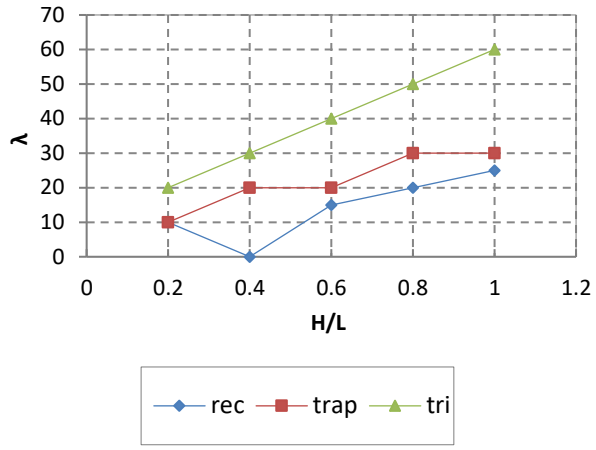

Fig. 8: λ as a function of depth ratio

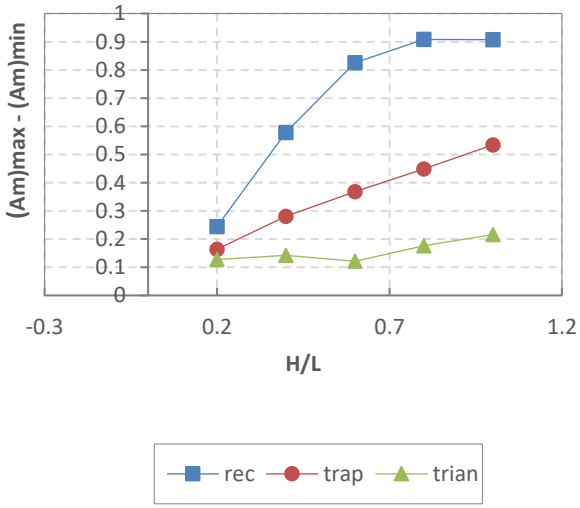

Fig. 9: The maximum change in amplification at the center of valleys as a function of depth ratio

Based on the information presented in this chapter and the concept of critical incidence angle:

1. The critical incidence angle for empty valley edges is different from the critical incidence angle defined in equation (3).
2. It appears that the critical incidence angle defined in equation (3) is close to that of present study (topographical critical incidence angle). Therefore, it is suggested to investigate topography within a range around the critical angle. Additionally, based on the amplification values in different topography shapes, it is recommended to consider this range to be larger, especially in cases where the effect of topography on vertical wave propagation is significant.
3. Generally, negative incidence angles are more critical than positive incidence angles, as observed in the results obtained from the Vittorito earthquake. In this earthquake, it was observed that on the hills, the slip was greater on one side compared to the other.

4. Conclusion

This study investigates the integrated effects of topography and the incidence angle of SV waves in empty valleys using the boundary element method. Valleys were modeled with rectangular, trapezoidal, and triangular shapes at depth ratios of 0.2, 0.4, 0.6, 0.8, and 1. The valleys were subjected to Seismic excitation of SV waves of a dominant frequency of 2 Hz. The incidence angles ranged from -90° to 90° with 10° increments. The results, presented in terms of total displacement amplification at various points across the valley width, involved the examination of various parameters such as depth ratio and valley shape in combination with the effect of the incidence wave angle. The critical points were examined and presented by different graphs. It was seen that the most critical point of all valleys is still the edge of the valley but the inclination of the incident wave could change the amplification factor for positive and negative angles with the same pattern but different magnitudes. The maximum amplification at the edge occurred at 10 degrees inclination angle for all cases and it was seen that the effect of angularity on amplification increases as the classical topography effect increases. In the center of the valleys, which is considered the least critical point, two different behaviors were observed. Finally, the study addresses the question of whether the presence of topography can alter the critical incidence angle of a half-space.

References

[1] Pagliaroli, A., Pergalani, F., Ciancimino, A., Chiaradonna, A., Compagnoni, M. A., De Silva, F., Foti, S., Giallini, S., Lanzo, G., Lombardi, F., Luzi, L., Macerola, L., Nocentini, M., Pizzi, A., Tallini, M., & Teramo, C. (2019). Site response analyses for complex geological and morphological conditions: relevant case-histories from 3rd level seismic microzonation in Central Italy. *Bulletin of Earthquake Engineering*, *18*(12), 5741–5777.

[2] Çetin, K. Ö., Papadimitriou, A. G., Altun, S., Pelekis, P., Unutmaz, B., Rovithis, E., Akgün, M., Klimis, N., Gündoğan, A. A., Ziotopoulou, K., Sezer, A., Kıncal, C., Ilgaç, M., Can, G., Çakır, E., Söylemez, B., Al-Suhaily, A., Elsaid, A., Zarzour, M., . . . Mylonakis, G. (2021). The role of site effects on elevated seismic demands and corollary structural damage during the October 30, 2020, M7.0 Samos Island (Aegean Sea) Earthquake. *Bulletin of Earthquake Engineering*, *20*(14), 7763–7792.

[3] Hartzell, S. H., Carver, D., & King, K. W. (1994). Initial investigation of site and topographic effects at Robinwood Ridge, California. *Bulletin of the Seismological Society of America*, *84*(5), 1336–1349.

[4] Bouchon, M., & Barker, J. S. (1996). Seismic response of a hill: The example of Tarzana, California. *Bulletin of the Seismological Society of America*, *86*(1A), 66–72.

[5] Spudich, P., Hellweg, M., & Lee, W. H. K. (1996). Directional topographic site response at Tarzana observed in aftershocks of the 1994 Northridge, California, earthquake: Implications for mainshock motions. *Bulletin of the Seismological Society of America*, *86*(1B), S193–S208.

[6] Athanasopoulos, G., Pelekis, P., & Leonidou, E. (1999). Effects of surface topography on seismic ground response in the Egion (Greece) 15 June 1995 earthquake. *Soil Dynamics and Earthquake Engineering*, *18*(2), 135–149.

[7] Bouckovalas, GD, Kouretzis, G. Review of soil and topography effects in the September 7, 1999 Athens (Greece) earthquake. In: Proceedings of the fourth international conference on recent advances in geotechnical earthquake engineering and soil dynamics and symposium in honor of Professor WD Liam Finn. San Diego, California; 2001.

[8] Trifunac, M. D., & Hudson, D. E. (1971). Analysis of the Pacoima dam accelerogram—San Fernando, California, earthquake of 1971. *Bulletin of the Seismological Society of America*, *61*(5), 1393–1411.

[9] Assimaki, D. (2005). Effects of Local Soil Conditions on the Topographic Aggravation of Seismic Motion: Parametric Investigation and Recorded Field Evidence from the 1999 Athens Earthquake. *Bulletin of the Seismological Society of America*, *95*(3), 1059–1089.

[10] Géli, L., Bard, P., & Jullien, B. (1988). The effect of topography on earthquake ground motion: A review and new results. *Bulletin of the Seismological Society of America*, *78*(1), 42–63.

[11] Ameri, G., Massa, M., Bindi, D., D'Alema, E., Gorini, A., Luzi, L., Marzorati, S., Pacor, F., Paolucci, R., Puglia, R., & Smerzini, C. (2009). The 6 April 2009 MW 6.3 L'Aquila (Central Italy) earthquake: strong-motion observations. *Seismological Research Letters*, *80*(6), 951–966.

[12] Biondi, G., & Maugeri, M. (2005). Seismic response analysis of Monte Po hill (Catania). In *WIT transactions on state-of-the-art in science and engineering*.

[13] Fukushima, Y., Irikura, K., Uetake, T., & Hisashi, M. (2000). Characteristics of Observed Peak Amplitude for Strong Ground Motion from the 1995 Hyogoken Nanbu (Kobe) Earthquake. *Bulletin of the Seismological Society of America*, *90*(3), 545–565.

[14] HB.Ozmen, An Investigation on Soil Amplification through Site Factors Used in Seismic Design Codes, Advances in Civil Engineering Volume 2023, Article ID 6858371, 11 pages

[15] Bard, P. (1997). Local effects of strong ground motion: Basic physical phenomena and estimation methods for microzoning studies.

[16] Lacave, C & Bard, Pierre-Yves & Koller, Martin. (1999). Microzonation: Techniques and examples. Block 15: Naturgefahren-Erdbebenrisiko

[17] Sánchez-Sesma, F. J., Palencia, V. J., & Luzón, F. (2004). Estimation of local site effects during earthquakes: An overview. *From Seismic Source to Structural Response: Contributions of Professor Mihailo D. Trifunac*, 44-70.

[18] Giallini, S., Pizzi, A., Pagliaroli, A., Moscatelli, M., Vignaroli, G., Sirianni, P., Mancini, M., & Laurenzano, G. (2020). Evaluation of complex site effects through experimental methods and numerical modelling: The case history of Arquata del Tronto, central Italy. *Engineering Geology*, *272*, 105646. https://doi.org/10.1016/j.enggeo.2020.105646

[19] Borcherdt, R. D. (1970). Effects of local geology on ground motion near San Francisco Bay. *Bulletin of the Seismological Society of America*, *60*(1), 29–61. https://doi.org/10.1785/bssa0600010029

[20] Bard, P. Y., & Riepl-Thomas, J. (2000). Wave propagation in complex geological structures and their effects on strong ground motion. *Wave motion in earthquake engineering*, 37-95.

[21] Andrews, D. J. (1986). Objective determination of source parameters and similarity of earthquakes of different size. *Earthquake source mechanics*, *37*, 259-267..

[22] Castro, R. R., Anderson, J. G., & Singh, S. K. (1990). Site response, attenuation and source spectra of S waves along the Guerrero, Mexico, subduction zone. *Bulletin of the Seismological Society of America*, *80*(6A), 1481-1503.

[23] Boatwright, J., Seekins, L. C., Fumal, T. E., Liu, H. P., & Mueller, C. S. (1991). Ground motion amplification in the Marina District. *Bulletin of the Seismological Society of America*, *81*(5), 1980-1997.

[24] Hartzell, S. H. (1992). Site response estimation from earthquake data. *Bulletin of the Seismological Society of America*, *82*(6), 2308-2327.

[25] Nogoshi, M., & Igarashi, T. (1970). On the Propagation Characteristics of Microtremor. *Journal of the Seismological Society of Japan*, *23*, 264-280.

[26] Nakamura, Y. (1989). A method for dynamic characteristics estimation of subsurface using microtremor on the ground surface. *Railway Technical Research Institute, Quarterly Reports*, *30*(1).

[27] Lermo, J., & Chávez-García, F. J. (1993). Site effect evaluation using spectral ratios with only one station. *Bulletin of the seismological society of America*, *83*(5), 1574-1594.

[28] Sylvette, B. C., Cécile, C., Pierre-Yves, B., Fabrice, C., Peter, M., Jozef, K., & Fäh, D. (2006). H/V ratio: a tool for site effects evaluation. Results from 1-D noise simulations. *Geophysical Journal International*, *167*(2), 827-837.

[29] Bonnefoy-Claudet, S., Köhler, A., Cornou, C., Wathelet, M., & Bard, P. Y. (2008). Effects of Love waves on microtremor H/V ratio. *Bulletin of the Seismological Society of America*, *98*(1), 288-300.

[30] Field, E. H., & Jacob, K. H. (1995). A comparison and test of various site-response estimation techniques, including three that are not reference-site dependent. *Bulletin of the seismological society of America*, *85*(4), 1127-1143.

[31] Guéguen, P., Cornou, C., Garambois, S., & Banton, J. (2007). On the limitation of the H/V spectral ratio using seismic noise as an exploration tool: application to the Grenoble valley (France), a small apex ratio basin. *Pure and applied geophysics*, *164*, 115-134.

[32] Poursartip, B., Fathi, A., & Tassoulas, J. L. (2020). Large-scale simulation of seismic wave motion: A review. *Soil Dynamics and Earthquake Engineering*, *129*, 105909.

[33] Lamb, H. (1904). On the Propagation of Tremors over the Surface of an Elastic Solid. *Proceedings of the royal society of London*, *72*, 128-130.

[34] Hisada, Y. (1994). An efficient method for computing Green's functions for a layered half-space with sources and receivers at close depths. *Bulletin of the Seismological Society of America*, *84*(5), 1456-1472.

[35] Hisada, Y. (1995). An efficient method for computing Green's functions for a layered half-space with sources and receivers at close depths (Part 2). *Bulletin of the Seismological Society of America*, *85*(4), 1080-1093.

[36] Garvin WW. Exact transient solution of the buried line source problem. Proc R Soc Lond Ser A Math Phys Sci 1956;234(1199):528–41.

[37] Thomson, W. T. (1950). Transmission of elastic waves through a stratified solid medium. *Journal of applied Physics*, *21*(2), 89-93.

[38] Haskell, N. A. (1953). The dispersion of surface waves on multilayered media*. *Bulletin of the Seismological Society of America*, *43*(1), 17–34.

[39] Haskell, N. A. (1960). Crustal reflection of plane SH waves. *Journal of Geophysical Research*, *65*(12), 4147-4150.

[40] Haskell, N. A. (1962). Crustal reflection of plane P and SV waves. *Journal of Geophysical Research*, *67*(12), 4751-4768.

[41] Huang, M., Cegla, F., & Lan, B. (2023). Stiffness matrix method for modelling wave propagation in arbitrary multilayers. *International Journal of Engineering Science*, *190*, 103888.

[42] Poursartip, B., Fathi, A., & Kallivokas, L. F. (2017). Seismic wave amplification by topographic features: A

parametric study. *Soil Dynamics and Earthquake Engineering*, *92*, 503-527.

[43] Alterman, Z., & Karal Jr, F. C. (1968). Propagation of elastic waves in layered media by finite difference methods. *Bulletin of the Seismological Society of America*, *58*(1), 367-398.

[44] Hill, N. R., & Levander, A. R. (1984). Resonances of low-velocity layers with lateral variations. *Bulletin of the Seismological Society of America*, *74*(2), 521-537.

[45] Moczo, P. (1989). Finite-difference technique for SH-waves in 2-D media using irregular grids—application to the seismic response problem. *Geophysical Journal International*, *99*(2), 321-329.

[46] Frankel, A., & Vidale, J. (1992). A three-dimensional simulation of seismic waves in the Santa Clara Valley, California, from a Loma Prieta aftershock. *Bulletin of the Seismological Society of America*, *82*(5), 2045-2074.

[47] Aki, K., & Larner, K. L. (1970). Surface motion of a layered medium having an irregular interface due to incident plane SH waves. *Journal of geophysical research*, *75*(5), 933-954.

[48] Bard, P. Y., & Bouchon, M. (1980). The seismic response of sediment-filled valleys. Part 1. The case of incident SH waves. *Bulletin of the seismological society of America*, *70*(4), 1263-1286.

[49] Bard, P. Y., & Bouchon, M. (1980). The seismic response of sediment-filled valleys. Part 2. The case of incident P and SV waves. *Bulletin of the Seismological Society of America*, *70*(5), 1921-1941.

[50] Geli, L., Bard, P. Y., & Jullien, B. (1988). The effect of topography on earthquake ground motion: a review and new results. *Bulletin of the Seismological Society of America*, *78*(1), 42-63.

[51] Bouchon, M. (1973). Effect of topography on surface motion. *Bulletin of the Seismological Society of America*, *63*(2), 615–632.

[52] Bard, P. Y. (1982). Diffracted waves and displacement field over two-dimensional elevated topographies. *Geophysical Journal International*, *71*(3), 731-760.

[53] Zhao, C., & Valliappan, S. (1993). Seismic wave scattering effects under different canyon topographic and geological conditions. *Soil Dynamics and Earthquake Engineering*, *12*(3), 129-143.

[54] Zhao, C., Valliappan, S., & Wang, Y. C. (1992). A numerical model for wave scattering problems in infinite media due to p-and sv-wave incidences. *International Journal for Numerical Methods in Engineering*, *33*(8), 1661-1682.

[55] Bravo, M. A., & Sanchez-Sesma, F. J. (1990). Seismic response of alluvial valleys for incident P, SV and Rayleigh waves. *Soil Dynamics and Earthquake Engineering*, *9*(1), 16-19.

[56] Moczo, P., Bystrický, E., Kristek, J., Carcione, J. M., & Bouchon, M. (1997). Hybrid modeling of P-SV seismic motion at inhomogeneous viscoelastic topographic structures. *Bulletin of the seismological Society of America*, *87*(5), 1305-1323.

[57] Zahradník, J., & Moczo, P. (1996). Hybrid seismic modeling based on discrete-wave number and finite-difference methods. *Seismic Waves in Laterally Inhomogeneous Media: Part 1*, 21-38.

[58] Ohtsuki, A., & Harumi, K. (1983). Effect of topography and subsurface inhomogeneities on seismic SV waves. *Earthquake Engineering & Structural Dynamics*, *11*(4), 441-462.

[59] Mossessian, T. K., & Dravinski, M. (1987). Application of a hybrid method for scattering of P, SV, and Rayleigh waves by near-surface irregularities. *Bulletin of the Seismological Society of America*, *77*(5), 1784-1803.

[60] Mossessian, T. K., & Dravinski, M. (1992). A hybrid approach for scattering of elastic waves by three-dimensional irregularities of arbitrary shape. *Journal of Physics of the Earth*, *40*(1), 241-261.

[61] Khair, K. R., Datta, S. K., & Shah, A. H. (1989). Amplification of obliquely incident seismic waves by cylindrical alluvial valleys of arbitrary cross-sectional shape. Part I. Incident P and SV waves. *Bulletin of the Seismological Society of America*, *79*(3), 610-630.

[62] Khair, K. R., Datta, S. K., & Shah, A. H. (1991). Amplification of obliquely incident seismic waves by cylindrical alluvial valley of arbitrary cross-sectional shape. Part II. Incident SH and Rayleigh waves. *Bulletin of the Seismological Society of America*, *81*(2), 346-357.

[63] Gatmiri, B., & Kamalian, M. (2002), "Two-dimensional transient wave propagation in an elastic saturated porous media by a hybrid FE/BE method," *fifth European conference of numerical methods in geotechnical, paris,*

[64] Gatmiri, B., & Kamalian, M. (2002). On the fundamental solution of dynamic poroelastic boundary integral equations in the time domain. *International Journal of Geomechanics*, *2*(4), 381-398.

[65] Gatmiri, B., Arson, C., & Nguyen, K. V. (2008). Seismic site effects by an optimized 2D BE/FE method I. Theory, numerical optimization and application to topographical irregularities. *Soil dynamics and earthquake engineering*, *28*(8), 632-645.

[66] Nguyen, K. V., & Gatmiri, B. (2007). Evaluation of seismic ground motion induced by topographic irregularity. *Soil dynamics and earthquake engineering*, *27*(2), 183-188.

[67] Eshraghi, H., & Dravinski, M. (1989). Scattering of plane harmonic SH, SV, P and Rayleigh waves by non-axisymmetric three-dimensional canyons: A wave function expansion approach. *Earthquake engineering & structural dynamics*, *18*(7), 983-998.

[68] Van Nguyen, K. (2005). *Étude des effets de site dus aux conditions topographiques et géotechniques par une méthode hybride éléments finis/éléments frontières* (Doctoral dissertation, Ecole des Ponts ParisTech).

[69] Gatmiri, B., Nguyen, K. V., & Dehghan, K. (2007). Seismic response of slopes subjected to incident SV wave by an improved boundary element approach. *International journal for numerical and analytical methods in geomechanics*, *31*(10), 1183-1195.

[70] Gatmiri, B., Maghoul, P., & Arson, C. (2009). Site-specific spectral response of seismic movement due to geometrical and geotechnical characteristics of sites. *Soil Dynamics and Earthquake Engineering*, *29*(1), 51-70.

[71] Razmkhah, A., Kamalian, M., & Sadrolddini, S. M. A. (2008, October). Time Domain Modeling of Topographic Effects on the Seismic Response of Slopes. In *Proceedings of the 12th International Conference of International Association for Computer Methods and Advances in Geomechanics, Goa, India* (pp. 2940-2947).

[72] Le Pense, S., Gatmiri, B., & Maghoul, P. (2011, July). Influence of soil properties and geometrical characteristics of sediment-filled valleys on earthquake response spectra. In *8th International Conference on Structural Dynamics (EURODYN 2011* (pp. 130-136).

[73] Gatmiri, B., & Foroutan, T. (2012). New criteria on the filling ratio and impedance ratio effects in seismic response evaluation of the partial filled alluvial valleys. *Soil Dynamics and Earthquake Engineering*, *41*, 89-101.

[74] Kamalian, M., Gatmiri, B., Sohrabi-Bidar, A., & Khalaj, A. (2007). Amplification pattern of 2D semi-sine-shaped valleys subjected to vertically propagating incident waves. *Communications in Numerical Methods in Engineering*, *23*(9), 871-887.

[75] Gatmiri, B., & Amini-baneh, D. (2014). Impact of geometrical and mechanical characteristics on the spectral response of sediment-filled valleys. *Soil Dynamics and Earthquake Engineering*, *67*, 233-250.

[76] Gatmiri, B., Amini-Baneh, D., Dorostkar, O., & Vakili, M. R. (2013). Practical recommendations of spectral response analysis in non-curved alluvial valleys using hybrid FE/BE method. *Journal of Multiscale Modelling*, *5*(02), 1350006.

Appendix A

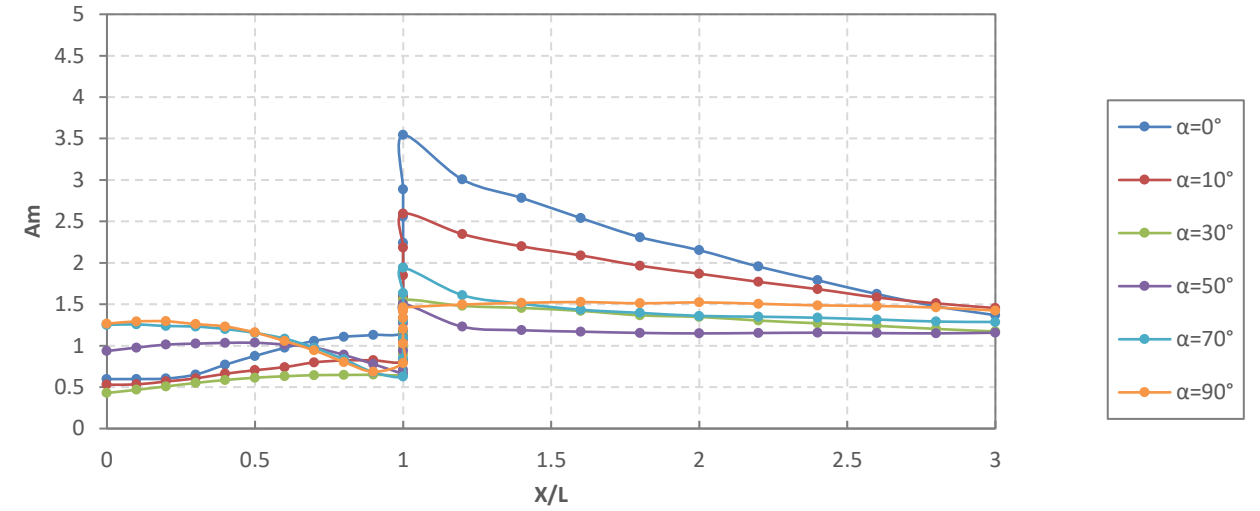

(a)

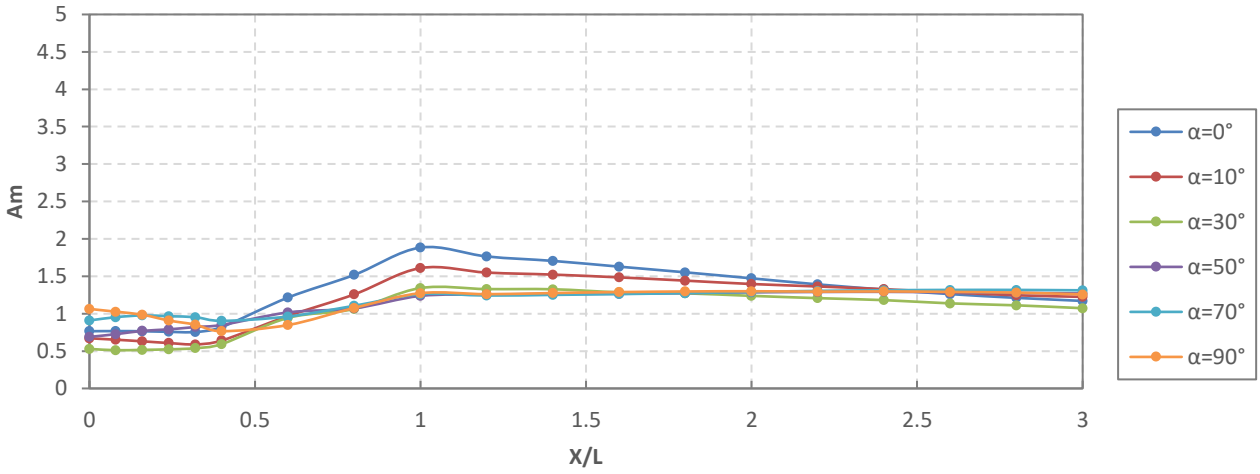

(b)

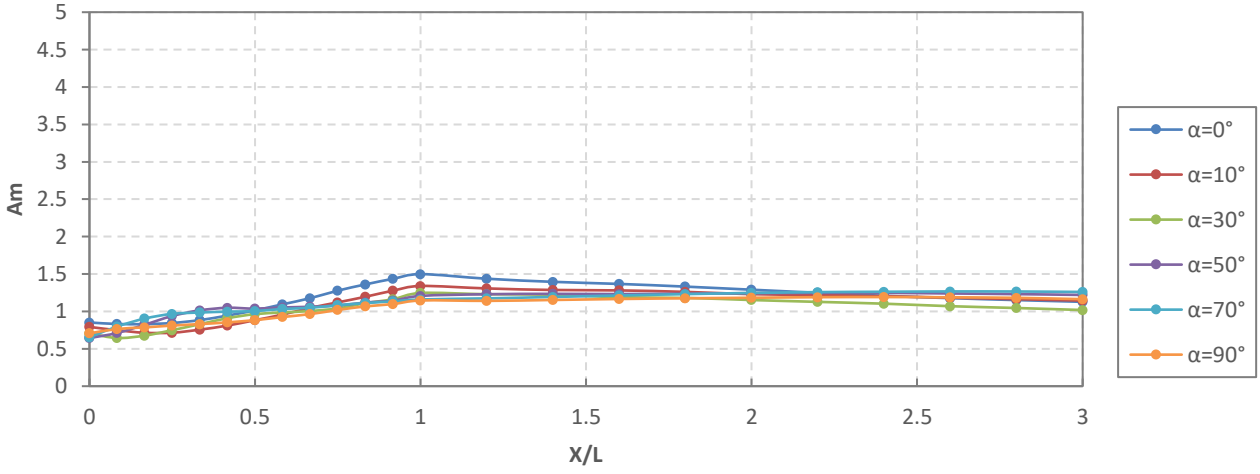

(c)

Fig. A. 1: Amplification of empty valleys with depth ratio of 1 as a function of $a > 0$, a) Rectangle, b) Trapezoid, c) Triangle.

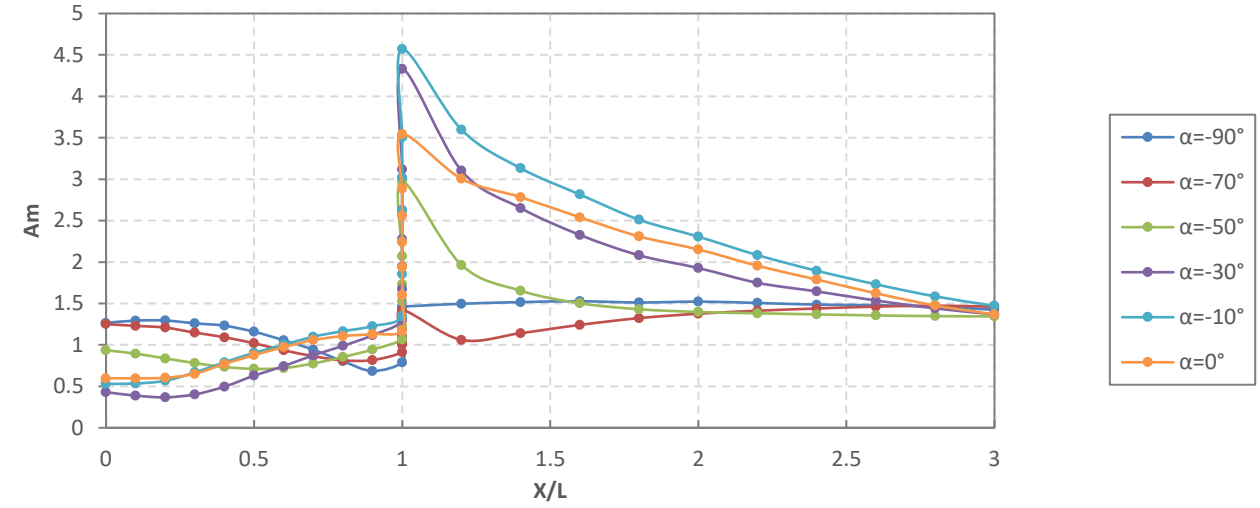

(a)

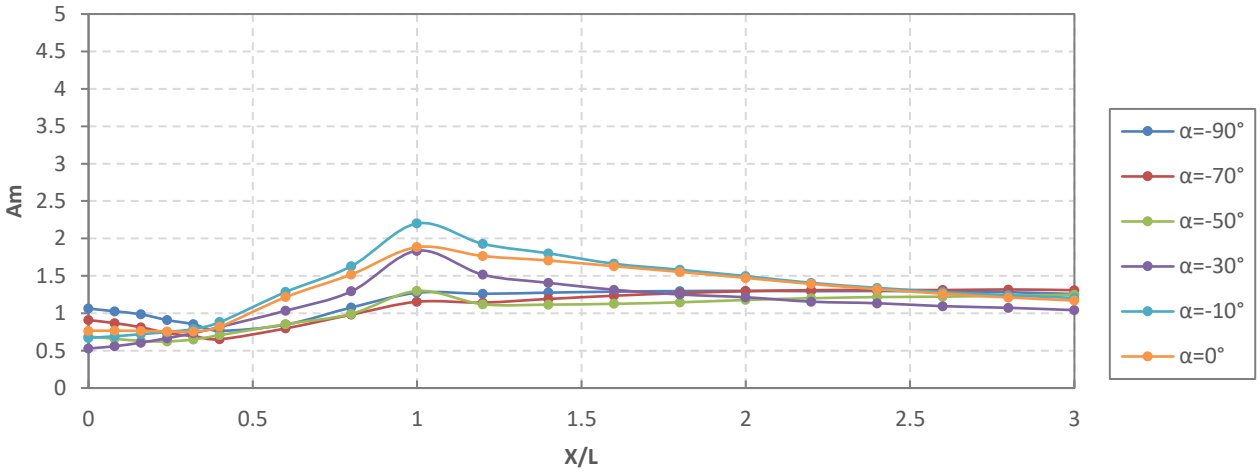

(b)

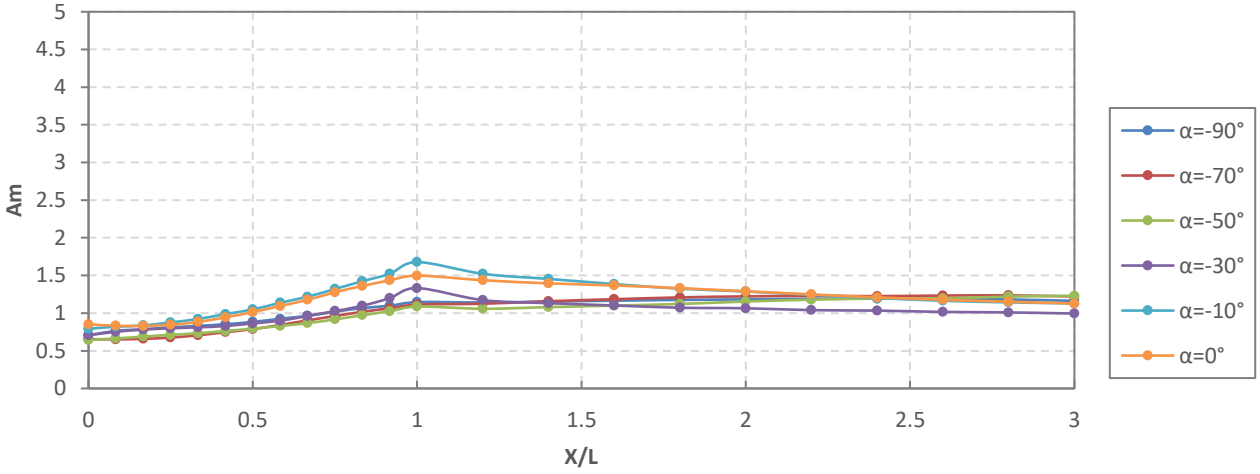

(c)

Fig. A. 2: Amplification of empty valleys with depth ratio of 1 as a function of $a < 0$, **(a)** Rectangle; **(b)** Trapezoid; **(c)** Triangle.

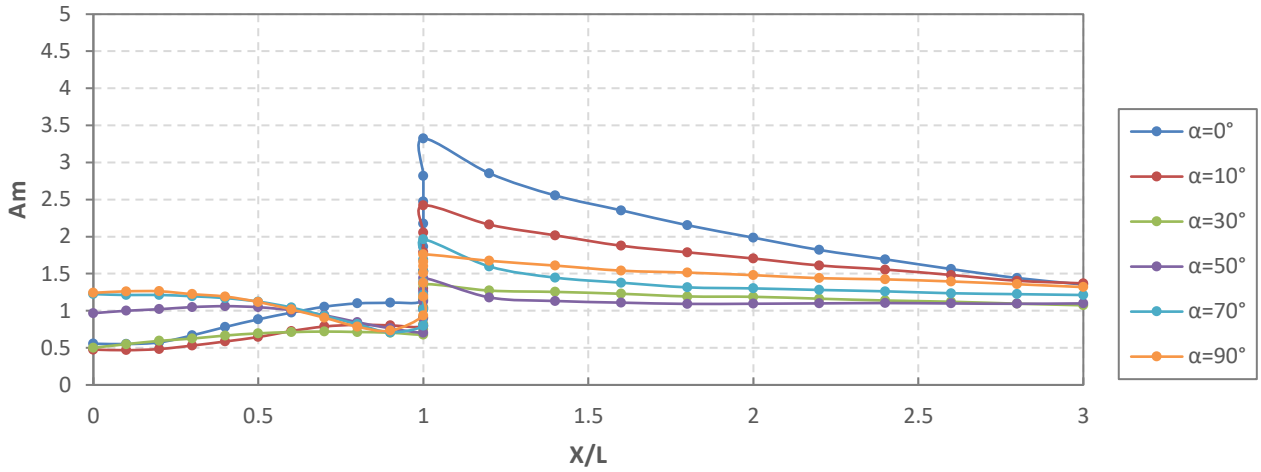

(a)

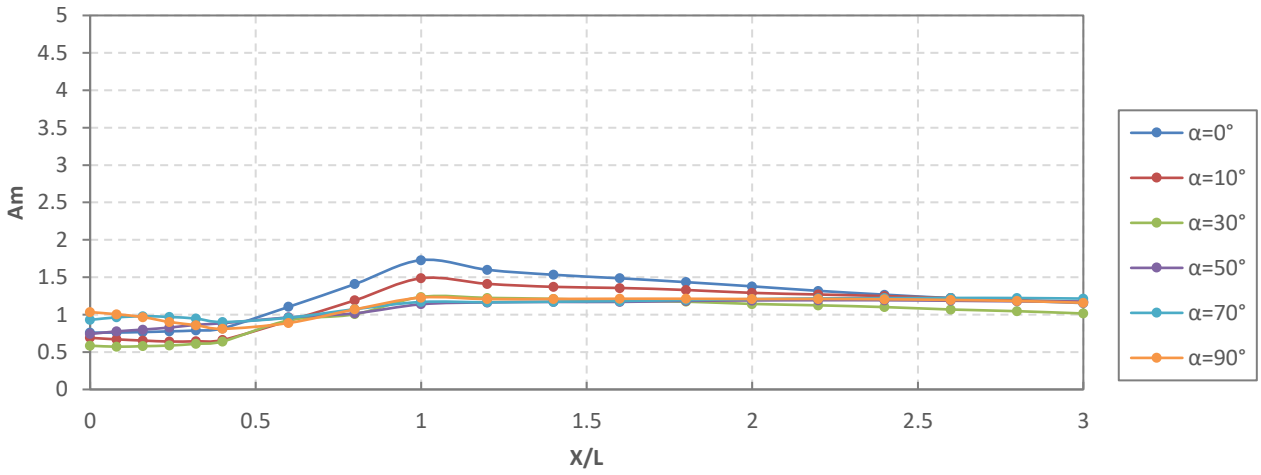

(b)

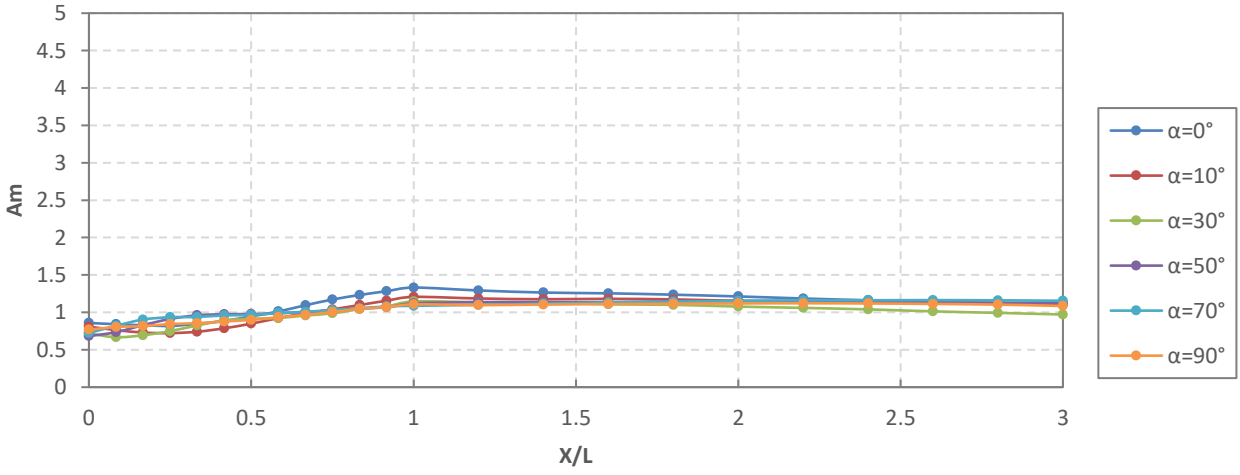

(c)

Fig. A. 3: Amplification of empty valleys with depth ratio of 0.8 as a function of $a > 0$, (a) Rectangle; (b) Trapezoid; (c) Triangle.

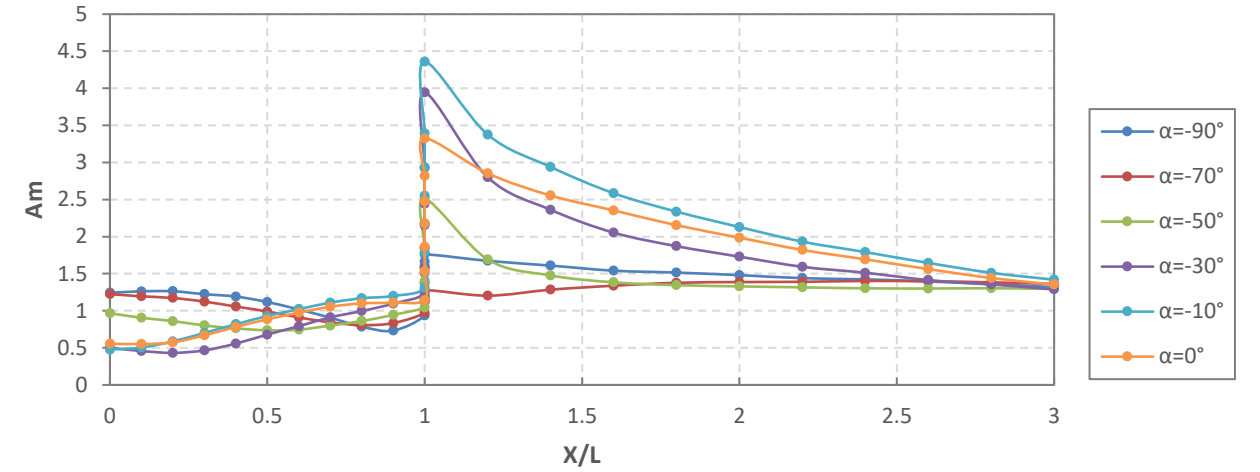

(a)

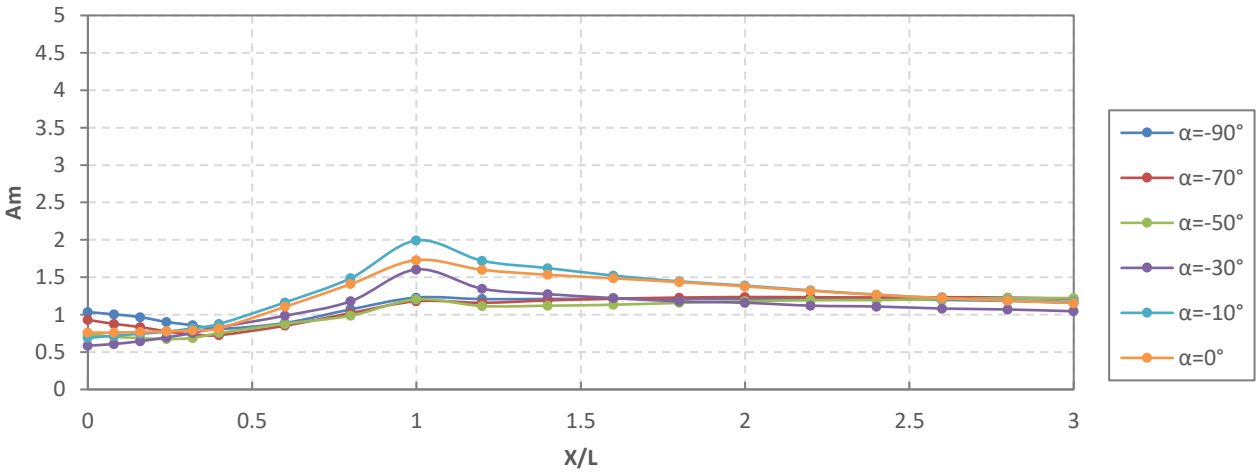

(b)

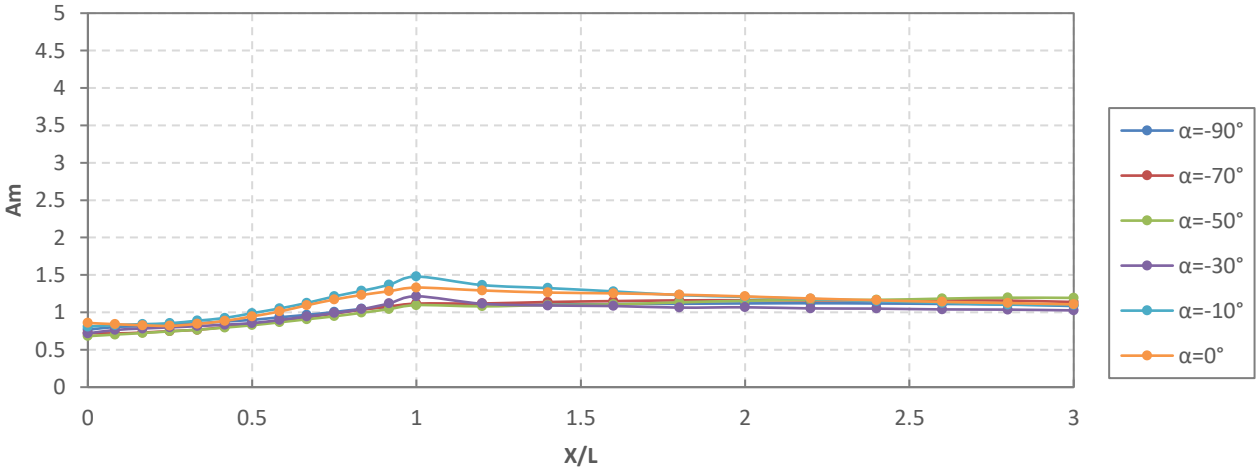

(c)

Fig. A. 4: Amplification of empty valleys with depth ratio of 0.8 as a function of $\alpha < 0$, (a) Rectangle; (b) Trapezoid; (c) Triangle.

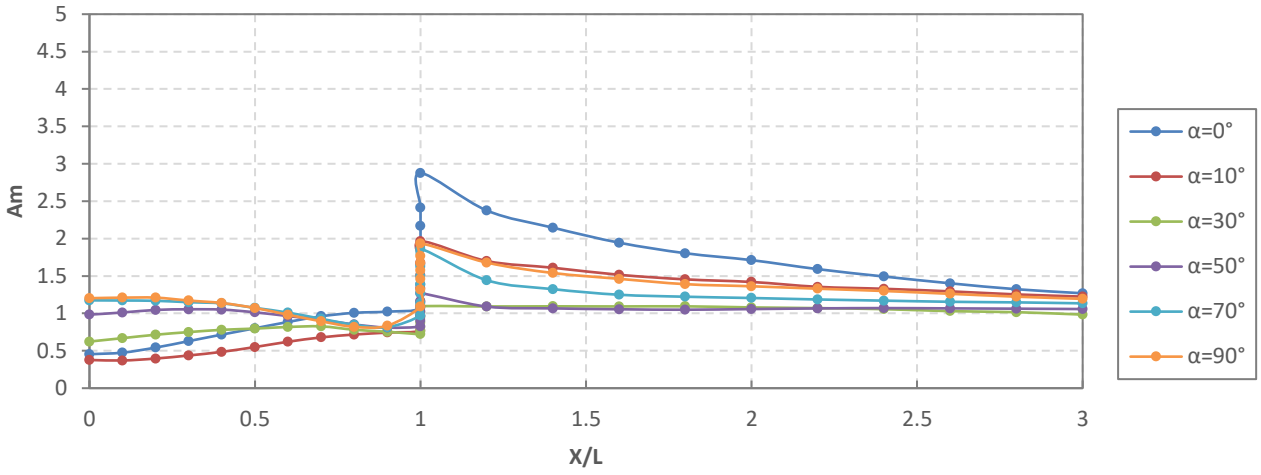

(a)

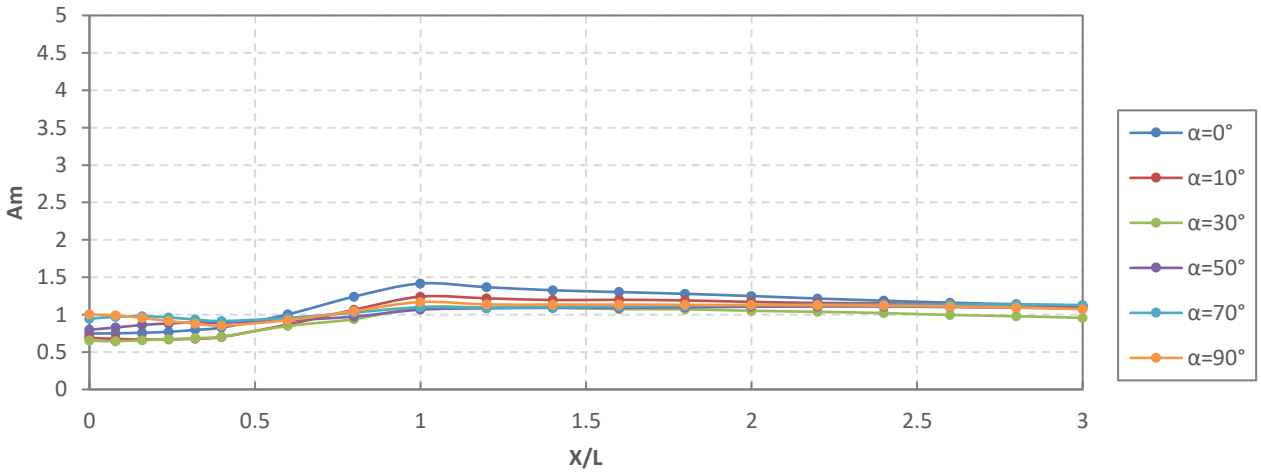

(b)

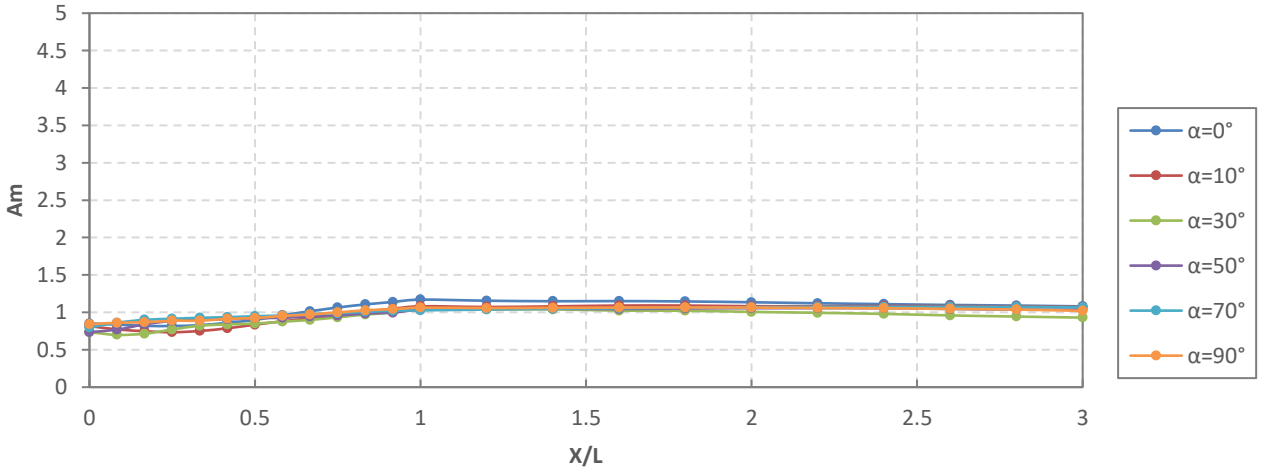

(c)

Fig. A. 5: Amplification of empty valleys with depth ratio of 0.6 as a function of $a > 0$, (a) Rectangle; (b) Trapezoid; (c) Triangle.

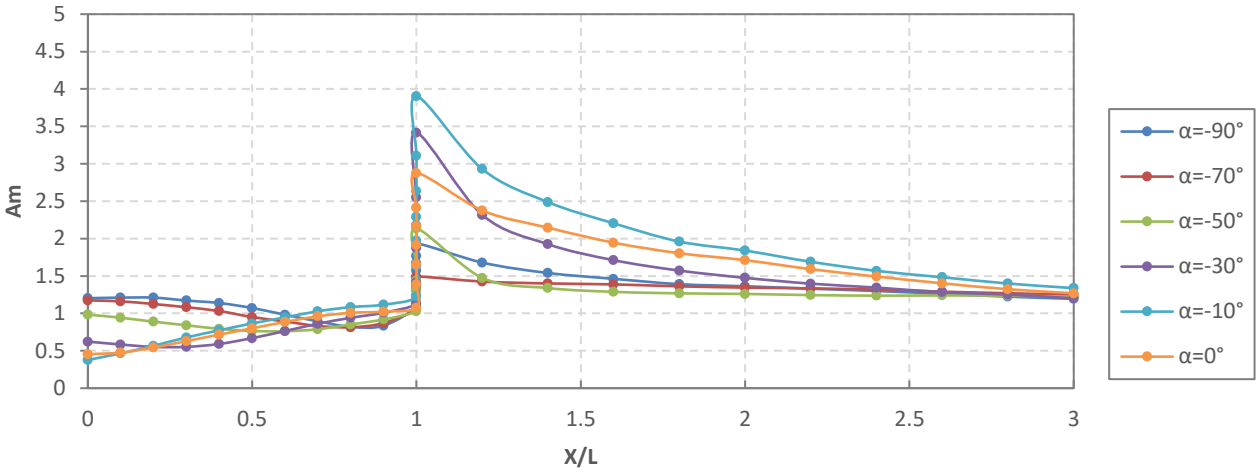

(a)

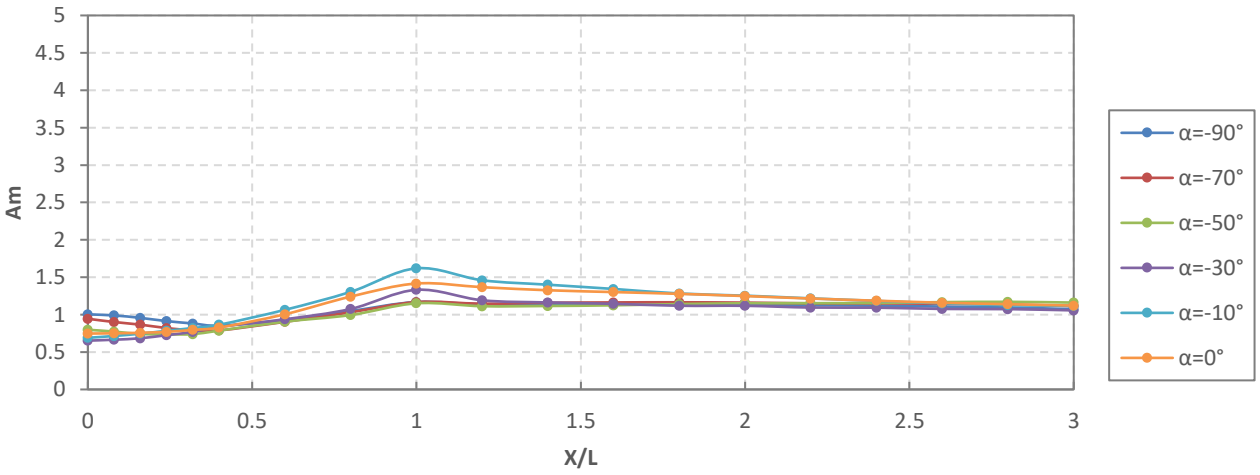

(b)

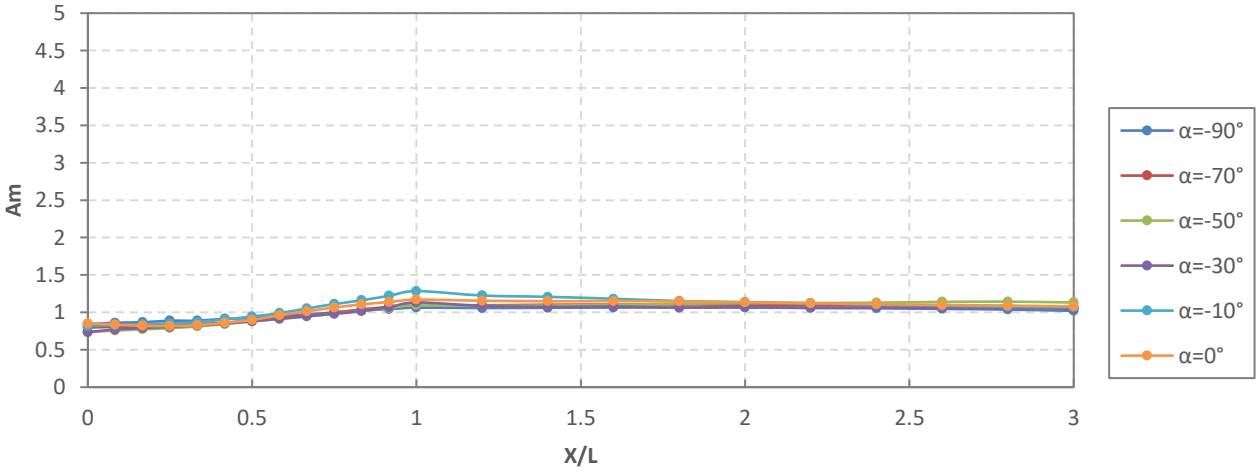

(c)

Fig. A. 6: Amplification of empty valleys with depth ratio of 0.6 as a function of $\alpha < 0$, (a) Rectangle; (b) Trapezoid; (c) Triangle.

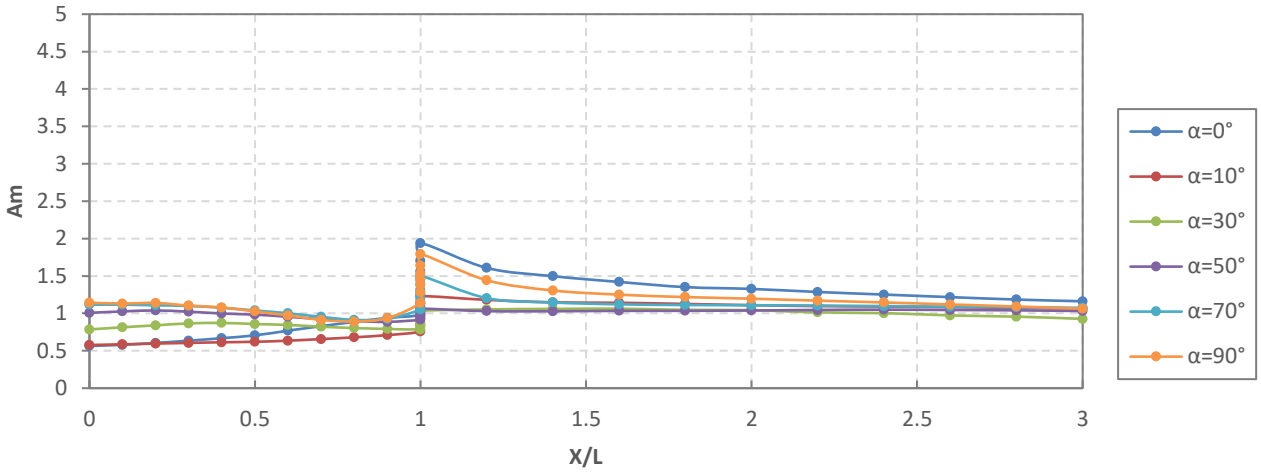

(a)

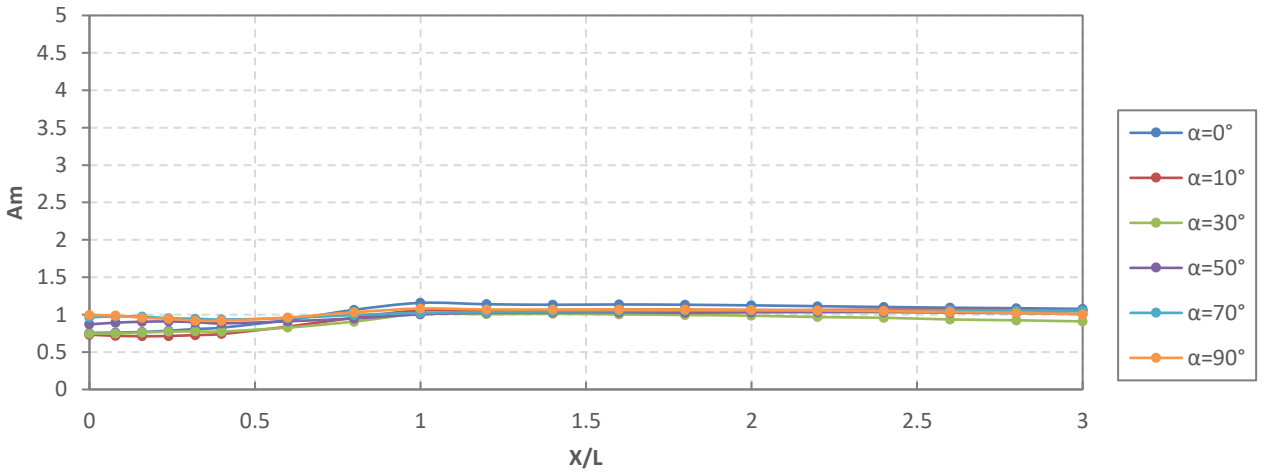

(b)

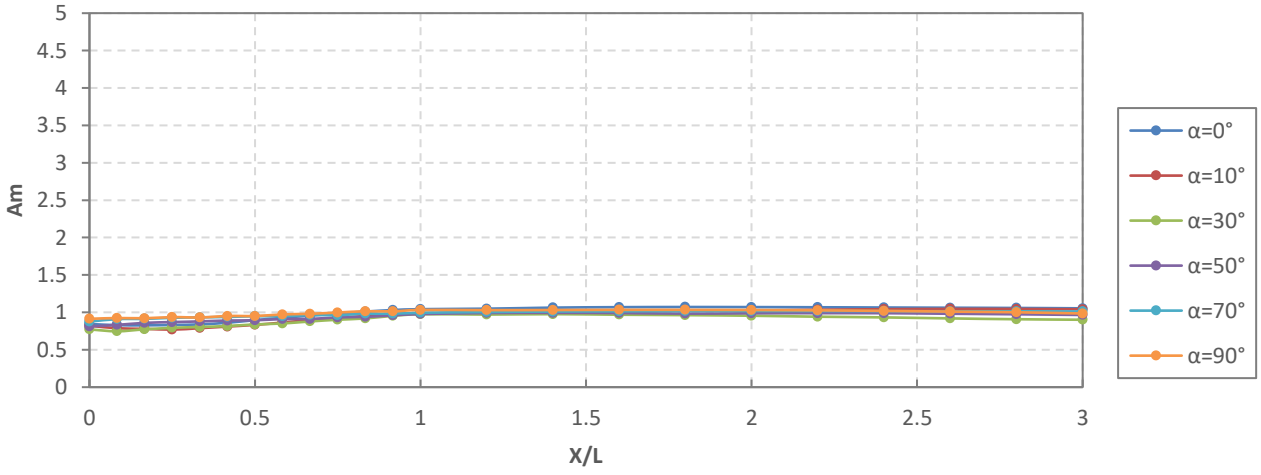

(c)

Fig. A. 7: Amplification of empty valleys with depth ratio of 0.4 as a function of $a > 0$, (a) Rectangle; (b) Trapezoid; (c) Triangle

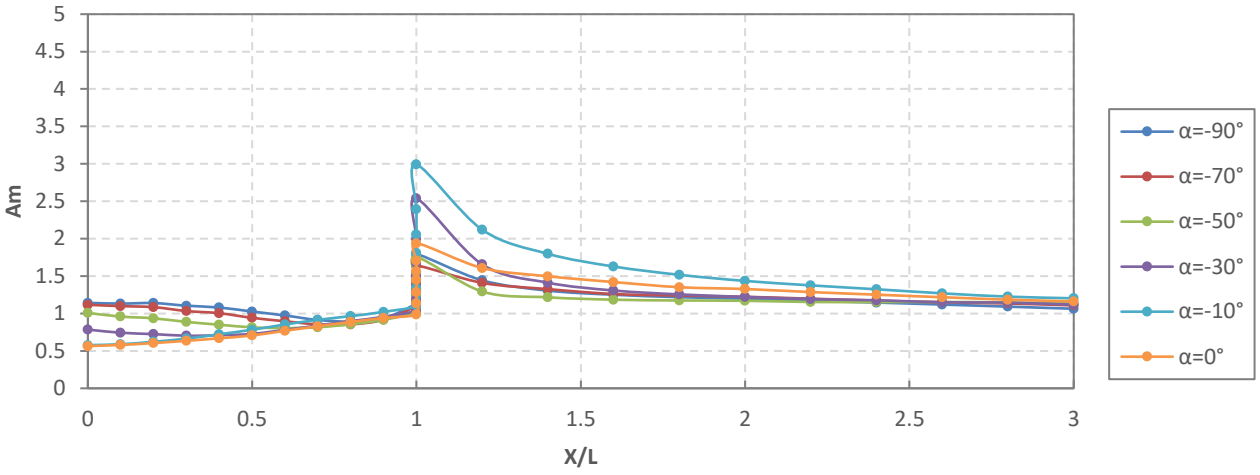

(a)

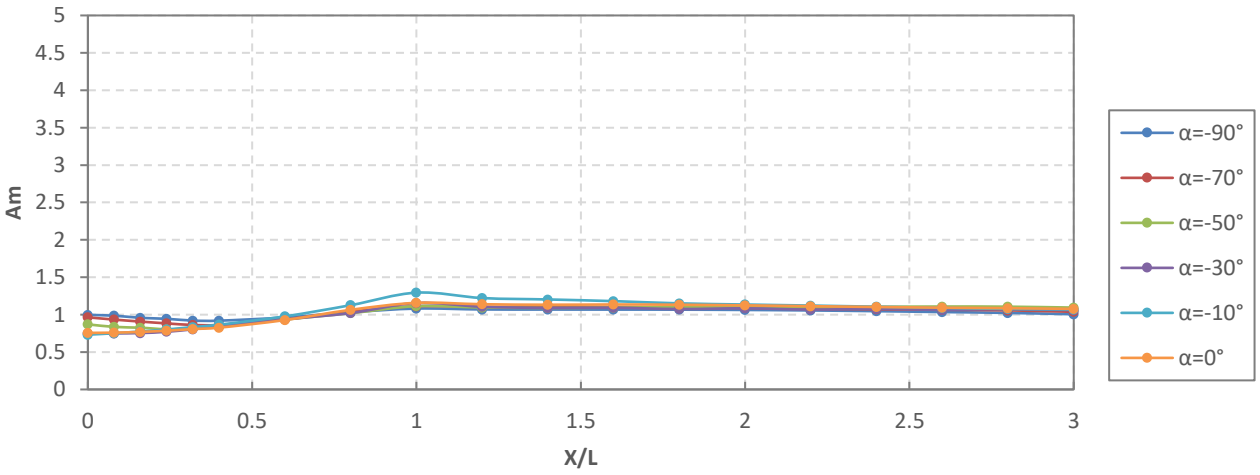

(b)

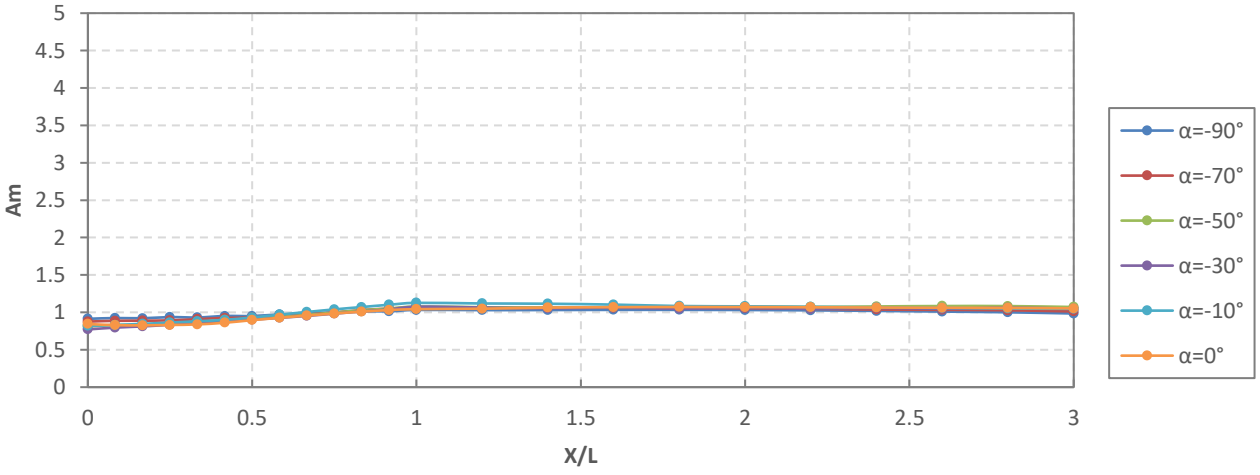

(c)

Fig. A. 8: Amplification of empty valleys with depth ratio of 0.4 as a function of $\alpha < 0$, (a) Rectangle; (b) Trapezoid; (c) Triangle

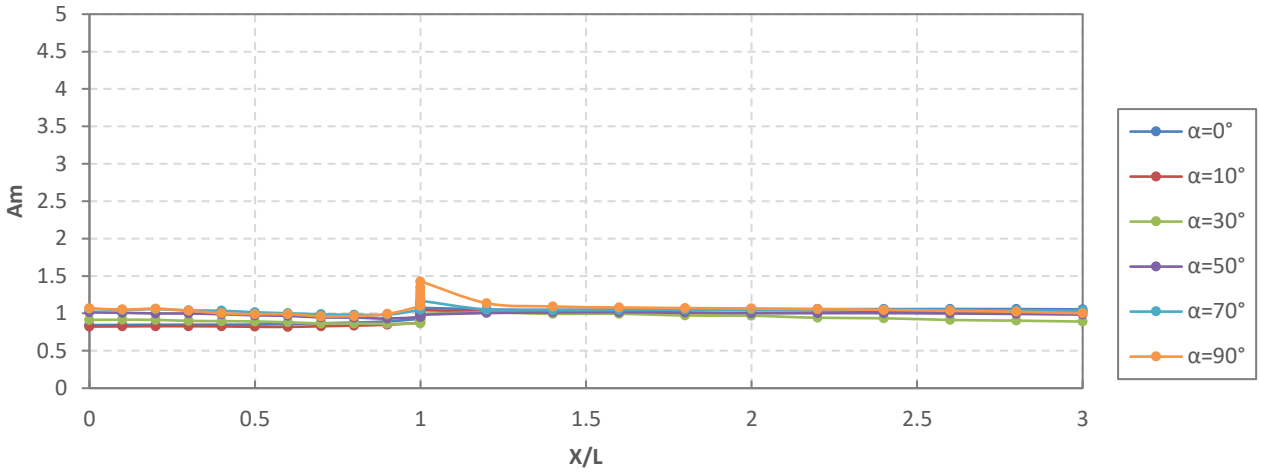

(a)

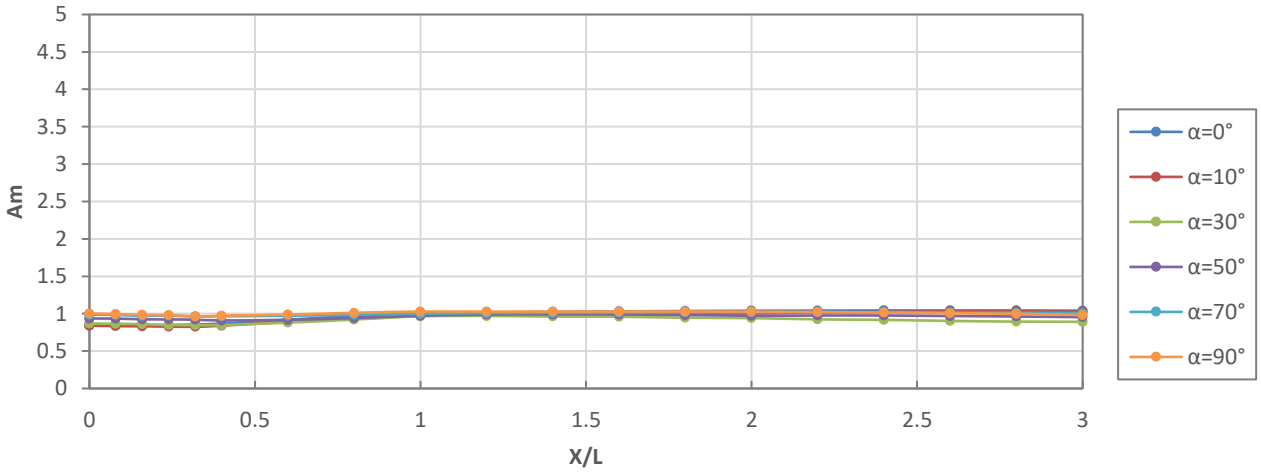

(b)

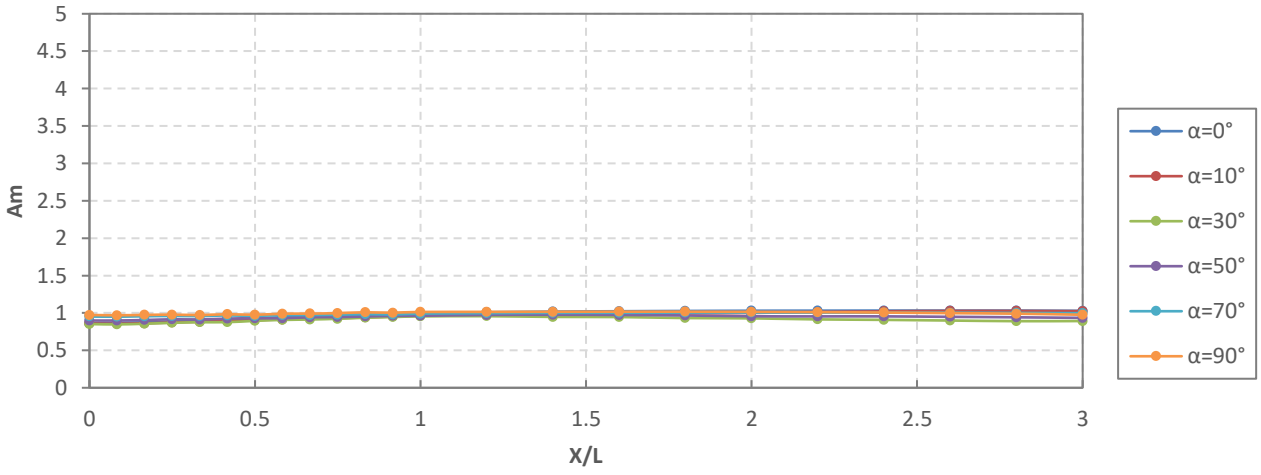

(c)

Fig. A. 9: Amplification of empty valleys with depth ratio of 0.2 as a function of $a > 0$, (a) Rectangle; (b) Trapezoid; (c) Triangle

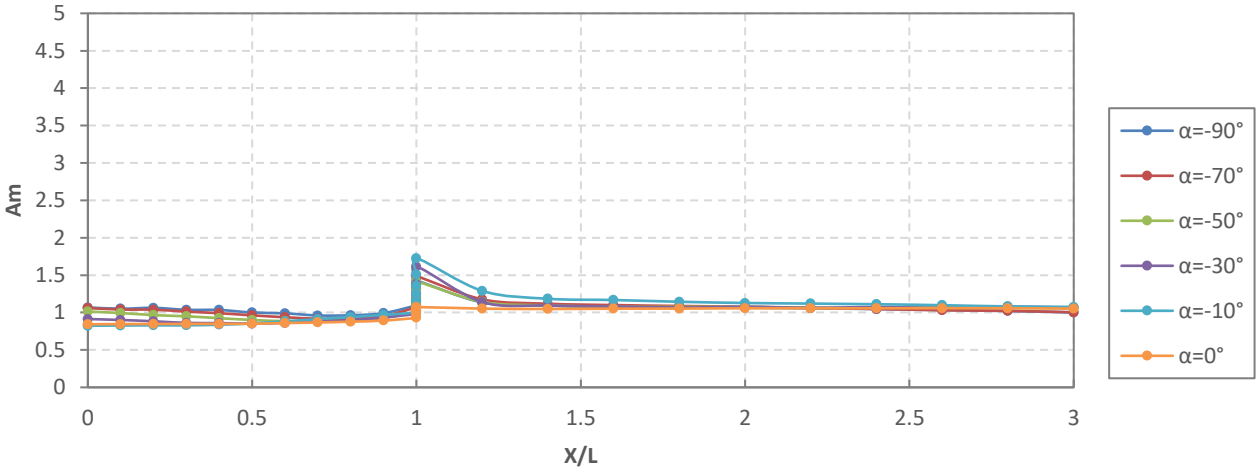

(a)

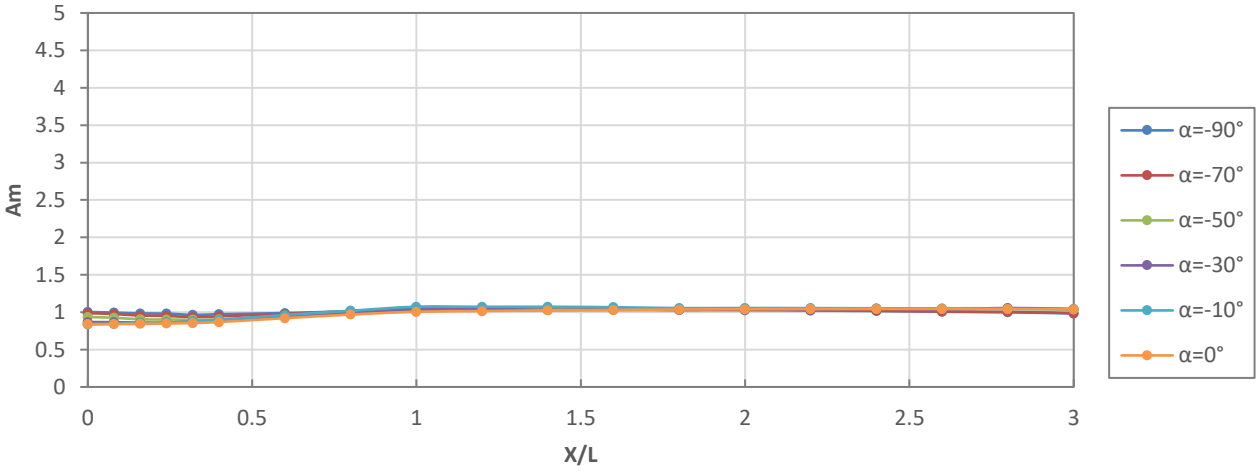

(b)

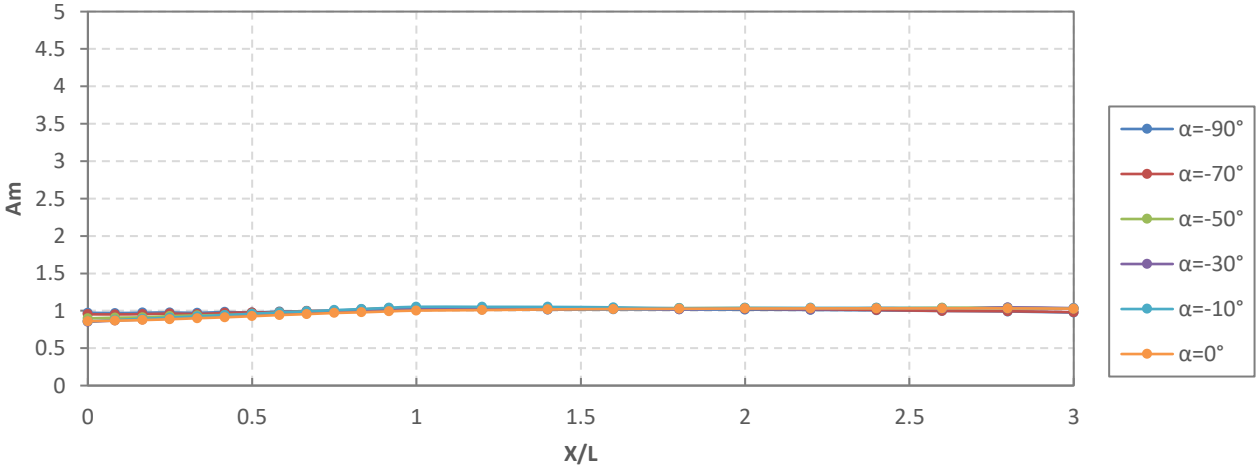

(c)

Fig. A. 10: Amplification of empty valleys with depth ratio of 0.2 as a function of $\alpha < 0$, (a) Rectangle; (b) Trapezoid; (c) Triangle